Apoptosis (2012) 17:852–870
DOI 10.1007/s10495-012-0705-6

ORIGINAL PAPER

Zinc oxide nanoparticles induce oxidative DNA damage and ROS-triggered mitochondria mediated apoptosis in human liver cells (HepG2)

Vyom Sharma · Diana Anderson · Alok Dhawan

Published online: 7 March 2012

Abstract The wide scale use of Zinc oxide (ZnO) nanoparticles in the world consumer market makes human beings more prone to the exposure to ZnO nanoparticles and its adverse effects. The liver, which is the primary organ of metabolism, might act as a major target organ for ZnO nanoparticles after they gain entry into the body through any of the possible routes. Therefore, the aim of the present study was to assess the apoptotic and genotoxic potential of ZnO nanoparticles in human liver cells (HepG2) and the underlying molecular mechanism of its cellular toxicity. The role of dissolution in the toxicity of ZnO nanoparticles was also investigated. Our results demonstrate that HepG2 cells exposed to 14–20 μg/ml ZnO nanoparticles for 12 h showed a decrease in cell viability and the mode of cell death induced by ZnO nanoparticles was apoptosis. They also induced DNA damage which was mediated by oxidative stress as evidenced by an increase in Fpg sensitive sites. Reactive oxygen species triggered a decrease in mitochondria membrane potential and an increase in the ratio of Bax/Bcl2 leading to mitochondria mediated pathway involved in apoptosis. In addition, ZnO nanoparticles activated JNK, p38 and induced $p53^{Ser15}$ phosphorylation. However, apoptosis was found to be independent of JNK and p38 pathways. This study investigating the effects of ZnO nanoparticles in human liver cells has provided valuable insights into the mechanism of toxicity induced by ZnO nanoparticles.

Keywords Zinc oxide nanoparticles · Human liver cells · Mechanism of toxicity · DNA damage · Apoptosis · MAPK · Oxidative stress

V. Sharma · A. Dhawan (✉)
Nanomaterial Toxicology Group, CSIR-Indian Institute of Toxicology Research, Mahatma Gandhi Marg, P.O. Box 80, Lucknow 226001, Uttar Pradesh, India
e-mail: dhawanalok@hotmail.com; alokdhawan@iitr.res.in; alok.dhawan@ahduni.edu.in

V. Sharma · D. Anderson
Division of Medical Sciences, School of Life Sciences, University of Bradford, Bradford BD7 1DP, West Yorkshire, UK

Present Address:
V. Sharma
Gillings School of Global Public Health, University of North Carolina, Chapel Hill, NC 27599, USA

A. Dhawan
Institute of Life Sciences, Ahmedabad University, 16/1 Vikram Sarabhai Marg, Opp IIM, Vastrapur, Ahmedabad 380015, Gujarat, India

Introduction

The field of nanotechnology is rapidly expanding with continuous development of nanomaterial based consumer products and their industrial applications. Nano forms of carbon based materials, metals, metal oxides and biopolymers are being used in several industries including diagnosis, drug delivery, cosmetics, sunscreens, food, paints, electronics, sports, imaging, etc. Zinc oxide nanoparticles (ZnO NPs) are one of the most abundantly used nanomaterials in cosmetics and sunscreens as they efficiently absorb UV light and also do not scatter visible light. This makes them transparent and more aesthetically acceptable compared to their bulk counterpart [1]. ZnO NPs are being used in the food industry as additives and in packaging due to their antimicrobial properties [2, 3]. They are also being explored for their potential use as fungicides in agriculture

[4], as anticancer drugs and biomedical imaging applications [5, 6].

The increased production and use of ZnO NPs enhances the probability of exposure in occupational and environmental settings. This has raised concerns in the public and scientific communities regarding their unanticipated and adverse health effects. Toxicity of ZnO NPs has been evaluated in different biological systems, such as, bacteria [7, 8], mammalian cells [9] and in vivo models [10]. In mammalian cells, the toxic effects of ZnO NPs such as membrane injury, inflammatory response, DNA damage and apoptosis have been demonstrated [11–13]. In some studies, the toxicity of ZnO NPs has been ascribed to the release of Zn^{2+} ions [14, 15]. However, studies have also shown that the toxicity of ZnO NPs is due to their particulate nature which may give rise to reactive oxygen species (ROS) [12, 16]. ROS generation is linked to DNA damage and cellular apoptosis [17, 18] and is also known to activate the mitogen activated protein kinase (MAPK) pathways which are important mediators of signal transduction and play a key role in regulating many cellular processes [19]. Despite the existing studies on the toxicity of ZnO NPs, the underlying molecular mechanism leading to toxicity remains largely unclear. Moreover, none of the studies, so far, have explored the adverse effects of ZnO NPs in human liver which is the primary organ of metabolism. ZnO NPs can be ingested directly when used in food, food packaging, drug delivery and cosmetics. Workers involved in the synthesis of ZnO NPs may be exposed by unintentional hand-to-mouth transfer of nanomaterials. When discharged into the environment accidently, these NPs may enter the human body through the food chain. In addition, some of the NPs can be swallowed into the gastrointestinal tract when they are expelled from the mucociliary system of the lungs after inhalation exposure [20]. NPs could be translocated from the lumen of the intestinal tract and blood into different organs like liver. Previous studies have shown that the NPs when administrated orally to mice accumulate in the liver and damage it [10, 21]. In another study, radiolabelled functionalized fullerenes were administrated intravenously to rats and a major percentage was found to be retained in the liver [22].

Since humans are directly exposed to ZnO NPs, it seems logical that the liver might act as a major target organ for ZnO NPs after they gain entry into the body through any of the possible routes. Therefore, the aim of the present study was to assess the cytotoxic and genotoxic potential of ZnO NPs in human liver cells (HepG2) and to understand the mechanism involved. To achieve this, we undertook a systematic study (Fig. 1) involving the assessment of cytotoxicity, ROS generation, lipid peroxidation, oxidative DNA damage and apoptosis. Levels of key signaling and apoptotic proteins along with the involvement of MAPK signaling pathways were analyzed. We also investigated if the toxicity was mediated by the Zn^{2+} ions liberated from NPs.

Materials and methods

Chemicals

Zinc oxide nanopowder (CAS No. 1314-13-2; purity >99%), neutral red dye, low melting point agarose (LMA), ethidium bromide (EtBr), Triton X-100, *N*-acetyl cysteine (NAC), Zinc chloride ($ZnCl_2$), SP600125, SB203580, vitamin C, vitamin E, Na-orthovanadate, Na-fluoride, Ponceau S stain and protease inhibitor cocktail were purchased from Sigma Chemical Co. Ltd. (St. Louis, MO, USA). Normal melting agarose (NMA), ethylenediaminetetraacetic acid (EDTA) disodium salt, and (3-(4, 5-dimethyl- thiazol-2-yl)-2, 5-diphenyl tetrazolium bromide (MTT) dye were purchased from Hi-media Pvt. Ltd. (Mumbai, India). Phosphate buffered saline (Ca^{2+}, Mg^{2+} free; PBS), minimal essential medium (MEM), trypsin–EDTA, fetal bovine serum (FBS), trypan blue, antibiotic and antimycotic solution (10,000 U/ml penicillin, 10 mg/ml streptomycin, 25 µg/ml amphotericin-B) were purchased from Gibco, USA. Formamidopyrimidine DNA glycosylase (Fpg) was kindly provided by Prof. Andrew Collins (Department of Nutrition, University of Oslo, Norway). All other chemicals were obtained locally in India and were of analytical reagent grade.

Particle characterization

ZnO NPs were suspended in complete minimal essential medium (CMEM; MEM supplemented with 10% FBS) at a concentration of 80 µg/ml and probe sonicated (Sonics & Material Inc., New Town, CT, USA) at 30 watt for 10 min (2.5 min on and 30 s off). Size and zeta potential were determined using dynamic light scattering and phase analysis light scattering in a Zetasizer Nano-ZS, Model ZEN3600 equipped with 4.0 mW, 633 nm laser (Malvern instruments Ltd., Malvern, UK).

Samples for transmission electron microscopy (TEM) analysis were prepared by drop coating a solution of ZnO NPs (8 µg/ml in Milli-Q) on carbon-coated copper grids. The films on the TEM grids were allowed to dry prior to measurement. TEM measurements were performed on a Tecnai^{TM} G2 Spirit (FEI, The Netherland) instrument operated at an accelerating voltage at 80 kV.

Cell culture and exposure to nanoparticles

The human hepatocarcinoma cell line (HepG2; obtained from the National Centre for Cell Sciences, Pune, India)

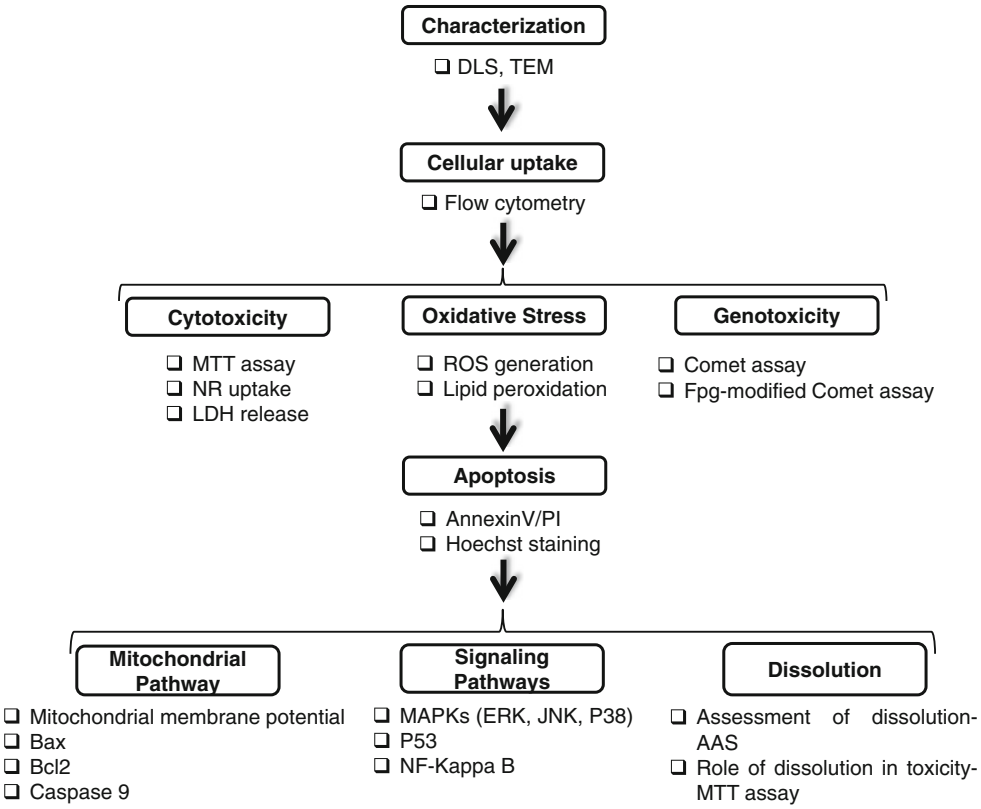

Fig. 1 Schematic diagram of the study design

was cultured in CMEM containing 10 ml/L of antibiotic and antimycotic solution at 37°C under a humidified atmosphere of 5% CO_2/95% air.

HepG2 cells were plated at a density of 10^5 cells/ml in a 96 well plate and 12 well plate for the cytotoxicity assays (MTT, neutral red uptake and lactate dehydrogenase) and other parameters (Comet assay, apoptosis, mitochondrial membrane potential), respectively and allowed to attach for 24 h before the addition of NPs suspension. A stock suspension of ZnO NPs (80 μg/ml) was prepared as described before and diluted to different concentrations (0.8, 2, 8, 14–20 μg/ml). Cells were then exposed to the above concentrations for varied lengths of time according to the experimental design.

To investigate the role of ROS and different signaling pathways the cells were pretreated with 1 mM NAC, SB203580 (20 μM), SP600125 (20 μM), 1.5 mM vitamin C (Ascorbic acid), 1.5 mM vitamin E (α-Tocopherol) and vitamin C + vitamin E for 2 h followed by simultaneous treatment of ZnO NPs with the respective inhibitor. After 24 h exposure, the cells were checked for cell viability by the MTT assay.

Cellular uptake of ZnO nanoparticles

The uptake of nanoparticles using flow cytometry was measured according to the method of Suzuki et al. [23]. The principle of this assay is that during the cellular uptake of non-fluorescent NPs, the forward-scattered (FSC) light remains constant in exposed and unexposed cells, while the intensity of side-scattered (SSC) light increases in proportion to the concentration of nanoparticles inside the cells. In the present study, 10^5 cells/ml were seeded in 6-well cell culture plates. After 24 h of seeding, the cells were exposed to ZnO nanoparticles (8, 14, 20 μg/ml) for 6 h. The culture medium containing nanoparticles was then removed and cells were harvested using 0.05% trypsin. The cells were then centrifuged at 250 g for 5 min. The supernatant was discarded and the pellet was re-suspended in 0.5 ml of PBS. The uptake of nanoparticles was measured by flow cytometer (FACS Canto™ II, BD Biosciences, San Jose, CA, USA) equipped with a 488 nm laser.

Cytotoxicity assays

MTT assay

The mitochondrial activity was assessed using the MTT assay following the method of Mosmann [24]. The cells were incubated for different time periods with ZnO NPs and for 4 h with MTT [3-(4,5-dimethylthiazoyl-2-yl)-2,5-diphenyltetrazolium bromide] dye. The medium from each well was discarded and the resulting formazon crystals were

solubilized by adding 200 µl of dimethylsulphoxide and quantified by measuring absorbance at 530 nm in a SYNERGY-HT multiwell plate reader, Bio-Tek (Winooski, USA) using KC4 software. The CC_{50} value of ZnO NPs at 24 h was calculated from MTT assay using the formula of Reed and Muench [25].

Neutral red uptake (NRU) assay

The neutral red uptake assay was done according to the method of Borenfreund and Puerner [26]. After the exposure, medium was discarded and 100 µl of neutral red dye (50 µg/ml) dissolved in serum free medium was added to each well. After incubation at 37°C for 3 h, cells were washed with a solution of 0.5% formaldehyde and 1% $CaCl_2$. The dye taken up by cells was dissolved in a medium containing 50% ethanol and 1% acetic acid in Milli-Q water. Absorbance was taken at 540 nm in a SYNERGY-HT multiwell plate reader, Bio-Tek (Winooski, USA) using KC4 software.

Lactate dehydrogenase (LDH) release

LDH activity in extracellular medium due to membrane damage was assessed by Tox-7 in vitro toxicology assay kit (Sigma-Aldrich Inc., St. Louis, MO, USA) using manufacturer's protocol. The resulting coloured compound was measured spectrophotometrically at 490 nm in a SYNERGY-HT multiwell plate reader, Bio-Tek (Winooski, USA) using KC4 software.

Oxidative stress parameters

Measurement of intracellular reactive oxygen species (ROS)

The level of intracellular ROS generation was estimated by the method of Wan et al. [27] using 2,7-dichlorofluorescein diacetate (DCFDA; Sigma, St Louis, MO, USA) dye. Cells were seeded in a 96-well black bottom plate (10^4 cells/well). After 24 h, the cells were exposed to ZnO NPs (8, 14, 20 µg/ml) for 6 h. Following exposure, the cells were washed twice with PBS and incubated with DCFDA dye (20 µM) for 30 min at 37°C. The reaction mixture was then replaced by 200 µl of PBS and fluorescence intensity was measured in a SYNERGY-HT multiwell plate reader, Bio-Tek (Winooski, USA) using KC4 software at excitation and emission wavelengths of 485 and 528 nm, respectively. The qualitative analysis of ROS generation was done using a microscope with a fluorescence attachment (DMLB, Leica, Germany).

Lipid peroxidation

The cells exposed to ZnO NPs were harvested in chilled PBS by scraping and washed twice with PBS at 4°C for 6 min at 1,500 rpm. The cell pellet was then sonicated at 15 W for 10 s (3 cycles) to obtain the cell lysate. The lipid peroxidation was estimated by Cayman's Chemicals Kit (USA) according to the manufacturer's protocol. Briefly, lipid hydroperoxide was extracted from the cell lysate into $CHCl_3$. Ferrous ions were added to the cell extract, which on reaction with lipid hydroperoxide yielded ferric ions. The resulting ferric ions were detected spectrophotometrically at 500 nm using thiocyanate ion as the chromogen. 13-HpODE (13-hydroperoxy-octadecadienoic acid) was used as a standard.

Genotoxicity assessment

Single cell gel electrophoresis (Comet) assay

The cells exposed to ZnO NPs (8, 14, 20 µg/ml) for 6 h were washed with serum free medium and harvested with 0.06% trypsin. The cells were re-suspended in culture medium supplemented with 10% fetal bovine serum and slides were prepared by the method as described by Bajpayee et al. [28]. Two slides were prepared from each well (one well/concentration) and kept overnight at 4°C in lysis solution (2.5 M NaCl, 100 mM EDTA, 10 mM Tris, pH10) with 1% Triton X-100 (added just before use). The slides were subjected to DNA unwinding for 20 min and subsequently electrophoresis was performed at 0.7 V/cm and 300 mA at 4°C for 25 min in freshly prepared electrophoresis buffer (1 mM EDTA sodium salt and 300 mM NaOH). The excess alkali was neutralized with Tris buffer (400 mM, pH 7.4) and slides were stained with 20 µg/ml ethidiumbromide (EtBr) and stored at 4°C in a humidified slide box until scoring. Slides were scored at a final magnification of 400× using an image analysis system (Komet 4.0, ANDOR technology, Belfast, UK) attached to a microscope (DMLB, Leica, Germany) equipped with a fluorescence attachment of a CCD camera. The Comet parameters used to measure DNA damage in the cells were Olive tail moment (OTM) and tail DNA (%). Images from 50 random cells (25 from each replicate slide) were analyzed for each experiment as per the guidelines [29]. The experiment (and not the cell) was used as the experimental unit for data analysis.

Fpg-modified Comet assay

To determine the induction of oxidized bases, the slides were immersed in two changes of enzyme buffer [40 mM

HEPES, 0.1 M KCl, 0.5 mM EDTA and 0.2 mg/ml bovine serum albumin (pH 8.0)] after lysis. Gels were then covered with 30 µl Fpg enzyme (1:3,000 dilution in enzyme buffer) and a cover slip and incubated in a humidified chamber for 30 min at 37°C [30]. The slides were processed as in the standard alkaline Comet assay [28].

Apoptosis

Annexin V-FITC/PI staining

Annexin V-FITC/PI staining was carried out by Annexin V-FITC apoptosis detection kit (Sigma, St Louis, MO, USA) as per the manufacturer's protocol. Briefly, the cells were harvested by trypsinization, washed with PBS and re-suspended in binding buffer (10 mM HEPES/NaOH, pH 7.5 containing 140 mM NaCl and 2.5 mM $CaCl_2$) at a concentration of 10^6 cells/ml. Annexin V-FITC (5 µl) and propidium iodide (10 µl) was added to 500 µl of cell suspension and incubated for 10 min in the dark at room temperature. The cells were immediately analyzed by flow cytometry (FACS Canto™ II, BD BioSciences, San Jose, CA, USA). Fluorescence emitted by Annexin V bound FITC and DNA-bound propidium iodide in each event was detected as green and red fluorescence, respectively. Results were analyzed by FACSDiva 6.1.2 software.

Hoechst staining

Apoptotic nuclear morphology was also assessed using Hoechst 33342 (Sigma, St Louis, MO, USA). Cells were fixed with 4% paraformaldelyde at room temperature for 30 min, and were washed and then stained with 2 µg/ml Hoechst 33342 at 37°C for 10 min. The cells were washed and the morphology was observed by fluorescence microscopy (DMLB, Leica, Germany).

Mitochondrial membrane potential assessment

Mitochondrial membrane potential ($\Delta\Psi_m$) was detected with the fluorescent probe 5,5′,6,6′-tetrachloro-1,1′,3,3′-tetraethylbenzimidazolcarbocyanine iodide (JC-1; Molecular probes, USA). Cells exposed to ZnO NPs were harvested by trypsinization and washed with PBS twice. The cells were incubated with 10 µM JC-1 for 15 min at 37°C, washed with PBS and re-suspended in PBS at a concentration of 10^6 cells/ml. The fluorescence intensity was measured at an excitation wavelength of 485 nm and an emission wavelength of 590 nm using flow cytometry (FACS Canto™ II, BD BioSciences, San Jose, CA, USA). For qualitative analysis, the cells were imaged for green and red fluorescence using a microscope with a fluorescence attachment (DMLB, Leica, Germany).

Western blot analysis

Cells treated with ZnO NPs were pelleted and lysed using CelLytic™ M Cell Lysis Reagent (Sigma, St. Louis, MO, USA) in the presence of Na-orthovanadate, Na-fluoride and protease inhibitor cocktail. The total protein concentration was measured by the Bradford method [31] and bovine serum albumin as the standard. Proteins (40 µg/lane) were resolved by the SDS-polyacrylamide gel electrophoresis and transferred to a nitrocellulose membrane. The membrane was blocked with 5% non fat milk for 1.5 h at room temperature and probed with anti-human primary antibodies (1:1,000) against β-actin, JNK, phospho-JNK, ERK1/2, phospho-ERK1/2, p38, phospho-p38, caspase-9, p53, phospho-p53(Ser15), Bcl2, Bax, nuclear factor kappa β (NF-kβ), (Cell Signaling Technology, Danvers, MA) for 1 h at room temperature followed by overnight incubation at 4°C. The membrane was then incubated for 1.5 h at room temperature with secondary anti-primary antibody conjugated to horseradish peroxidase (Calbiochem, USA). The protein bands were visualized by enhanced chemiluminescence (Super Signal West Pico chemiluminescent reagent, Pierce, Rockford, IL) and densitometry was done using the Scion Image program (Scion Corporation, Fredrick, MD, USA). β-actin served as the protein loading control.

Effect of dissolution on the cytotoxicity induced by ZnO NPs

Zinc ions released from ZnO NPs were evaluated for their cytotoxicity. Cell culture medium containing ZnO NPs at a concentration of 20 µg/ml was incubated at 37°C for 3, 6, 12 and 24 h. Thereafter, the NPs suspension was centrifuged at 20,000 g (4°C) for 30 min to remove the NPs and the resulting supernatant was collected. Cell culture medium without NPs but subjected to the same conditions was used as the blank control. The Zn content in the supernatant was measured by an atomic absorption spectrophotometer (ZEEnit 700 P, Analytikjena, Germany). Before analysis, the atomic absorption spectrophotometer (AAS) was calibrated every time by running at least three standard concentrations (0.25, 0.5 and 1 mg/L) of zinc.

The cells were incubated with the supernatant for 6, 12 and 24 h and the cell viability was assessed by the MTT assay as described before. In other experiment, the cells were treated with $ZnCl_2$ equimolar in amount to the Zn content as determined by the AAS in the supernatant to evaluate the contribution of Zn^{2+} towards ZnO NP toxicity. The cytotoxicity was assessed after 6, 12 and 24 h exposure by the MTT assay.

Statistical analysis

Results were expressed as the mean ± SEM and data were analyzed by means of one way analysis of variance (ANOVA) with the Dunnett post hoc test to determine significance relative to the unexposed control using SPSS v. 16.0 software (SPSS Inc., Chicago, IL, USA). In all cases, $p < 0.05$ was considered significant.

Results

Particle characterization

The mean hydrodynamic diameter and zeta potential of the ZnO NPs in CMEM as determined by the DLS measurement was 267 nm and −12 mV, respectively (Fig. 2a–b). The average size measured by TEM was 30 nm (Fig. 2c).

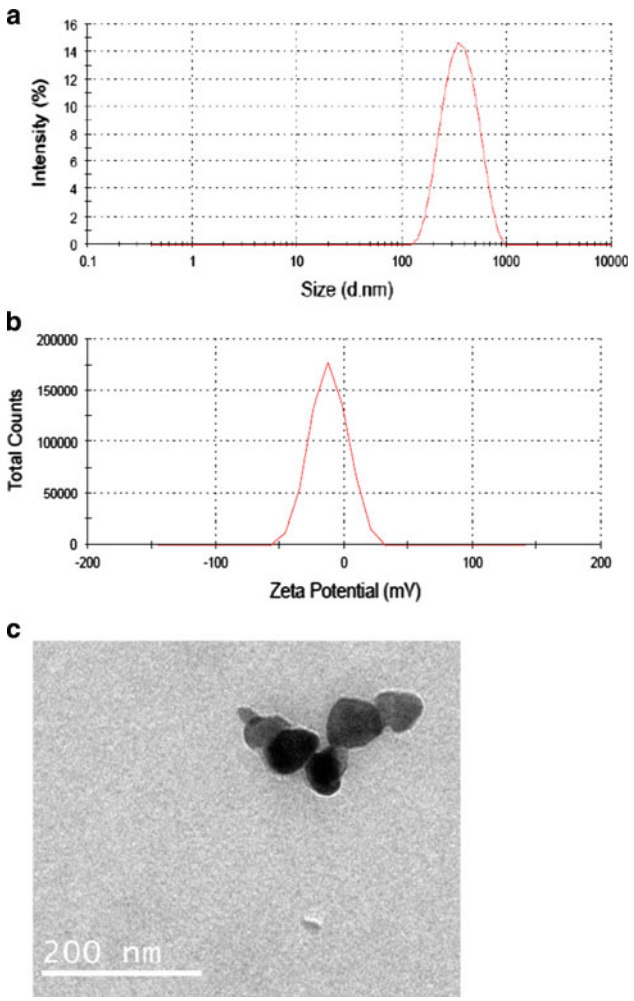

Fig. 2 Characterization of ZnO NPs; **a** Hydrodynamic diameter; **b** Zeta potential **c** TEM photomicrograph of ZnO NPs

Cellular uptake of nanoparticles

Cells treated with ZnO NPs showed a significant increase in the SSC-A mean. After 6 h exposure, the cells showed an SSC-A mean of 33,928 and 38,158 at 14 and 20 μg/ml, respectively as compared to the control cells (17,947; Fig. 3).

Cytotoxicity of ZnO nanoparticles

The cytotoxicity of ZnO NPs in HepG2 cells was evaluated by the MTT, NRU and LDH assays. HepG2 cells were exposed to ZnO NPs (0.8–20 μg/ml) for 6, 12 and 24 h. The MTT and NRU results demonstrated a concentration and time dependent cytotoxicity after exposure to ZnO NPs (Fig. 4a–b). The percentage mitochondrial activity (relative to control) observed after 12 h exposure at concentrations of 14 and 20 μg/ml was 80 and 74%, respectively with a further decrease to 53 and 43% after 24 h exposure. The CC_{50} value of ZnO NPs at 24 h was 14.5 μg/ml as calculated from the MTT assay.

The results of the NRU assay showed a similar concentration and time dependent response with a loss in cell viability at 14 and 20 μg/ml after 12 and 24 h exposure (Fig. 4b).

A significant ($p < 0.05$) LDH leakage was observed at 14 and 20 μg/ml after 24 and 12 h exposure, respectively (Fig. 4c).

Measurement of intracellular ROS

The cells exposed to ZnO nanoparticles (14 and 20 μg/ml) for 6 h showed a significant ($p < 0.05$) increase in the ROS generation. This was evident by a 31% increase (at 20 μg/ml) in the DCF fluorescence when measured qualitatively as well as quantitatively (Table 1; Fig. 5a–b).

Effect of ZnO nanoparticles on lipid peroxidation

Lipid peroxidation was examined by measuring hydroperoxide concentration. A statistically significant ($p < 0.05$) increase in hydroperoxide formation was observed only at the higher concentration (20 μg/ml) after 6 h exposure to ZnO NPs (Table 1).

DNA damage

The cell viability in the Comet assay exceeded 90% for all experimental groups before and after the treatment as assessed by the Trypan blue dye exclusion assay (data not shown).

A significant induction ($p < 0.05$) in DNA damage was observed in cells exposed to ZnO NPs for 6 h at 14 and

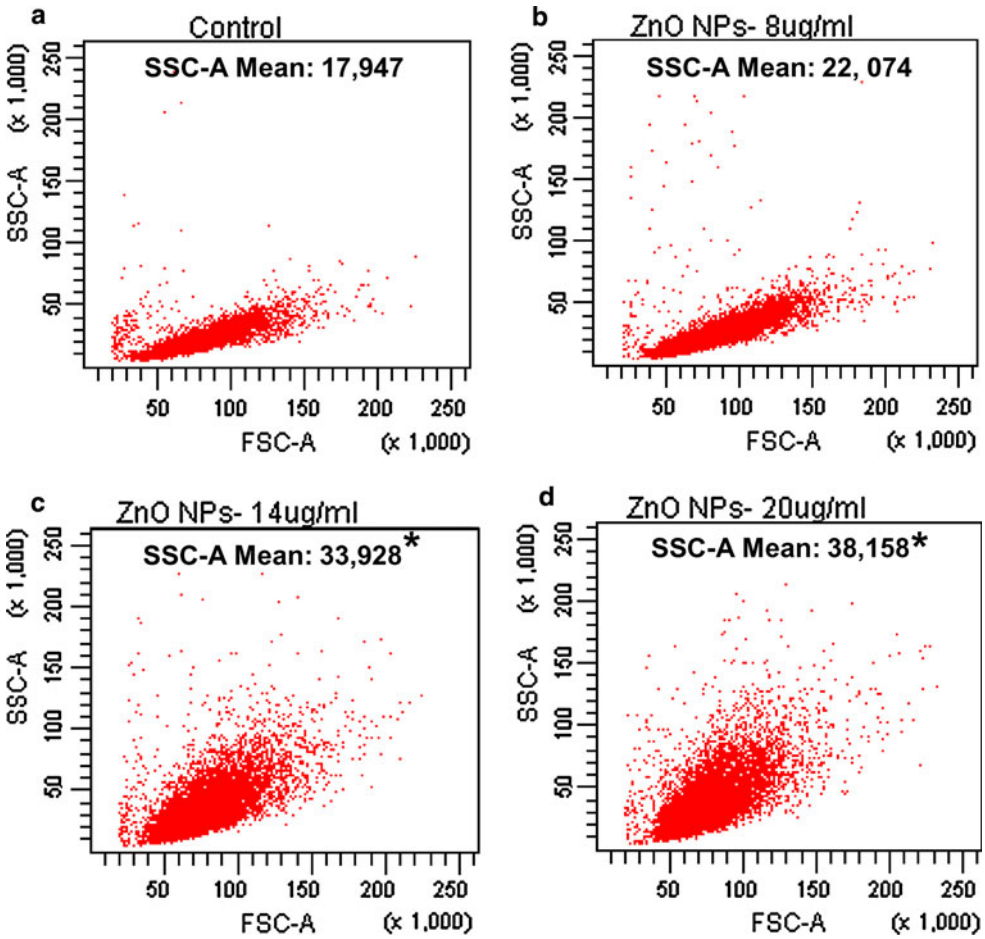

Fig. 3 Cellular uptake of ZnO NPs in HepG2 cells as assessed by the flow cytometry, **a** Control cells (**b–d**) Cells exposed to ZnO NPs

20 μg/ml concentrations compared to control cells in the standard alkaline Comet assay as evident by the Comet assay parameters i.e., Olive tail moment (arbitrary unit) and % tail DNA (Table 2). Moreover, in the Fpg modified Comet assay, the OTM values of the cells treated with 14 and 20 μg/ml ZnO NPs were significantly higher than the respective OTM values observed in the standard alkaline Comet assay suggesting the oxidative DNA damage. Additionally, cells exposed to the same concentrations of ZnO NPs revealed a significant ($p < 0.05$) increase in Fpg sensitive sites compared to control cells incubated with the Fpg enzyme (Table 2). To further confirm the involvement of oxidative stress, the level of Fpg sensitive sites were evaluated in the cells exposed to 20 μg/ml ZnO NPs in the presence of NAC. The results revealed a protective effect of NAC (0.75 mM and 1 mM) on the oxidative DNA damage as evident by a reduction in Fpg sensitive sites (Fig. 5c).

Apoptosis

Flow cytometry analysis was conducted using Annexin V-FITC/PI staining to investigate the mode of cell death induced by ZnO NPs. HepG2 cells were treated with 14 and 20 μg/ml ZnO NPs for 12 h. The control cells were not stained with Annexin V-FITC and propidium iodide. However, the cells treated with 14 and 20 μg/ml ZnO NPs for 12 h showed 8.1 and 12.8% apoptotic cells respectively (Fig. 6a–c).

Apoptosis was further confirmed by employing Hoechst 33342 staining. Stained control and ZnO NP treated cells were examined for nuclear morphology. The control cells had round and homogenously stained nuclei but cells treated with ZnO NPs (20 μg/ml) for 12 h showed marked DNA condensation and apoptotic bodies, characteristic of apoptosis (Fig. 6d–e).

Mitochondrial membrane potential ($\Delta\psi_m$) analysis

The cells treated with ZnO NPs for 12 h showed a marked decrease in $\Delta\psi_m$ evident by a shift in JC-1 fluorescence from red to green (Fig. 7a–b). There were 18.8% depolarized cells at 20 μg/ml as compared to the control cells (9.7%). Healthy cells with functional mitochondria showed red JC-1-aggregates which were detected in FL2 channel, while apoptotic cells with impaired mitochondria

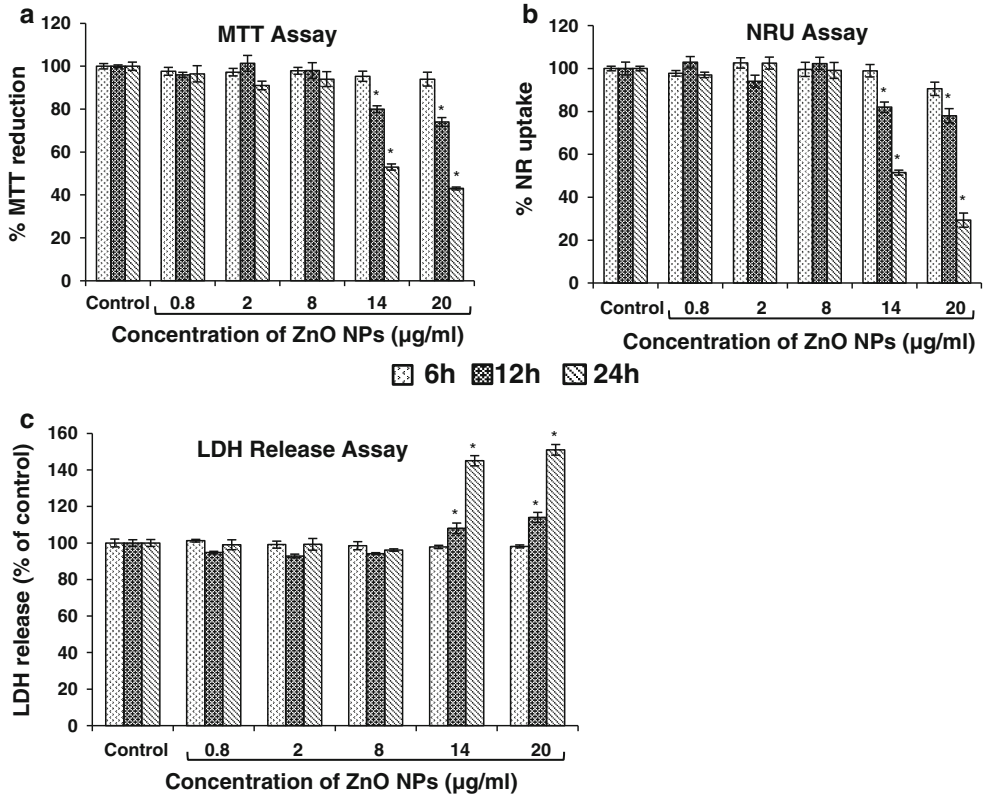

Fig. 4 Cytotoxic effect of ZnO NPs in HepG2 cells as assessed by **a** MTT assay; **b** Neutral red uptake assay; **c** Lactate dehydrogenase release assay. Data are expressed as the percentage viability of cells exposed to ZnO NPs relative to control cells and are mean ± SEM of triplicates. *$p < 0.05$, compared to control

Table 1 Effect of ZnO NPs on the ROS generation and lipid peroxidation in HepG2 cells after 6 h exposure

Concentrations	ROS generation (% of control)	Hydroperoxide concentration (nmol)
Control	100 ± 7	1.5 ± 0.05
ZnO NPs (8 μg/ml)	102 ± 5	1.4 ± 0.08
ZnO NPs (14 μg/ml)	116 ± 8	1.8 ± 0.04
ZnO NPs (20 μg/ml)	131 ± 5*	2.6 ± 0.03*

Values represent mean ± SE of three experiments

* $p < 0.05$ when compared to control using one way ANOVA

containing green JC-1 monomers were detected in the FL1 channel. When examined by fluorescent microscopy, the control cells showed an intense red fluorescence and weak green fluorescence. However, the cells treated with ZnO NPs exhibited a bright green fluorescence with a marked decrease in red fluorescence indicating a loss of MMP (Fig. 7c).

Analysis of key apoptotic and signaling proteins

The levels of key apoptotic and signaling proteins were examined in cells exposed to ZnO NPs for 9 h by Western blotting (Fig. 8). The cells showed modulation of Bax and Bcl2 protein expression levels with an increase in Bax levels and a corresponding decrease in Bcl2. A significant decrease in the procaspase-9 levels and an appearance of a cleavage product at 37kD was observed (Fig. 8). A 2.4 fold increase in the levels of phosphorylated $p53^{Ser15}$ was observed without any significant change in the levels of p53 (Fig. 8). No change in NF-kβ levels were observed on exposure to ZnO NPs.

Effect of ZnO NPs on MAPK phosphorylation

The effect of ZnO NPs on the phosphorylation of extracellular signal-regulating kinase (ERK1/2), stress activated protein kinase (SAPK)/Jun-N-terminal kinase (JNK), and p38 kinase in HepG2 cells was determined by Western blotting (Fig. 9a–c). A 2.2 fold increase in the phosphorylated JNK was observed at 20 μg/ml with no change in JNK proteins. Similarly, there was a 2.4 fold upregulation of phosphorylated p38 expression without any modulation of p38 expression. No changes in phospho-ERK and ERK levels were observed on exposure to ZnO NPs. Interestingly, p38 and JNK phosphorylation was completely prevented in the presence of NAC.

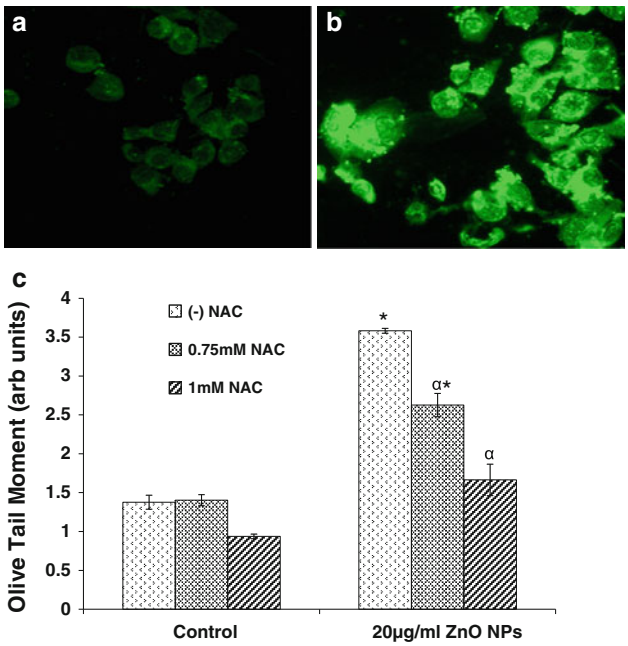

Fig. 5 Photomicrographs showing generation of the intracellular reactive oxygen species using DCFDA dye in HepG2 cells **a** Control cells; **b** Cells exposed to ZnO NPs for 6 h showing increase in fluorescence (Magnification ×200); **c** Effect of *N*-acetyl cysteine (NAC) on ZnO NP induced oxidative DNA damage in HepG2 cells; Data represent mean ± SEM of three experiments. $*p < 0.05$ when compared to control using one way ANOVA in Fpg-modified Comet assay. $^{\alpha}p < 0.05$ when compared to "(−) NAC" at the same concentration using the Student '*t*' test

Effect of NAC, SP600125, SB203580, vitamin C and vitamin E on the toxicity induced by ZnO nanoparticle

To determine the role of ROS and other signaling pathways in ZnO NP induced cell death, HepG2 cells were treated with ZnO NPs (20 μg/ml) in the presence of NAC (antioxidant), vitamin C, vitamin E, SP600125 (JNK inhibitor) and SB203580 (p38 inhibitor). The effect on cell viability was measured by the MTT assay. The presence of NAC completely abolished the cytotoxic effect of ZnO NP and showed cell viability similar to control cells even after 24 h of exposure (Fig. 10). Similar protective effect was shown by another antioxidant vitamin C as well as the simultaneous presence of vitamin C and vitamin E. However, addition of vitamin E (lipid peroxidation inhibitor), SP600125 (JNK inhibitor) and SB203580 (p38 inhibitor) did not provide any protection from ZnO NP induced cell death in HepG2 cells (Fig. 10).

Further, the presence of NAC significantly ($p < 0.05$) decreased the number of depolarized cells (Fig. 11a) as indicated by the JC-1 fluorescence in MMP analysis. Annexin V-FITC/PI and Hoechst 33342 staining indicated that NAC was able to protect cells from ZnO NP induced apoptosis (data not shown). Bax/Bcl2 modulation and $p53^{Ser15}$ phosphorylation was also noticeably inhibited by NAC addition (Fig. 11b).

Effect of dissolution on the cytotoxicity induced by ZnO NPs

The cells exposed to ZnO NP supernatant for 6, 12 and 24 h showed the same cell viability as that of control cells in MTT assay (Fig. 12a).

The AAS analysis of the supernatant revealed a Zn^{2+} of 1.2 ppm (18.46 μM) for all time periods (Fig. 12b). The cells were further treated with a soluble Zn salt- $ZnCl_2$ at an equivalent Zn mass dose (18 μM) for 6, 12 and 24 h and the cytotoxicity was assessed by the MTT assay. The assay revealed no decrease in cell viability on 6, 12 and 24 h exposure to $ZnCl_2$ (Fig. 12c).

Discussion

The present study reveals the effects of ZnO nanoparticles on human liver cells and provides significant insight into the possible mechanism through which ZnO nanoparticles exert their toxic effects on these cells. Our results demonstrate the cytotoxic and genotoxic potential of ZnO NPs

Table 2 Induction of DNA strand breaks and oxidative DNA damage in human liver cells after 6 h exposure to ZnO nanoparticles as evident by the Comet parameters

Concentrations	OTM (arbitrary unit)		Tail DNA (%)	
	Fpg (−)	Fpg (+)	Fpg (−)	Fpg (+)
Control	0.87 ± 0.14	1.21 ± 0.15	5.75 ± 0.88	7.19 ± 0.46
ZnO NPs (8 μg/ml)	1.00 ± 0.08	1.32 ± 0.19	6.80 ± 0.38	8.62 ± 0.79
ZnO NPs (14 μg/ml)	1.68 ± 0.19*	2.25 ± 0.15*$^{\alpha}$	8.90 ± 0.76*	11.00 ± 0.62*
ZnO NPs (20 μg/ml)	2.17 ± 0.20*	4.09 ± 0.05*$^{\alpha}$	11.15 ± 0.11*	14.51 ± 0.55*$^{\alpha}$

Values represent mean ± SE of three experiments

* $p < 0.05$ when compared to control using one way ANOVA

$^{\alpha}$ $p < 0.05$ when compared to Fpg (−) at the same concentration using Student '*t*' test

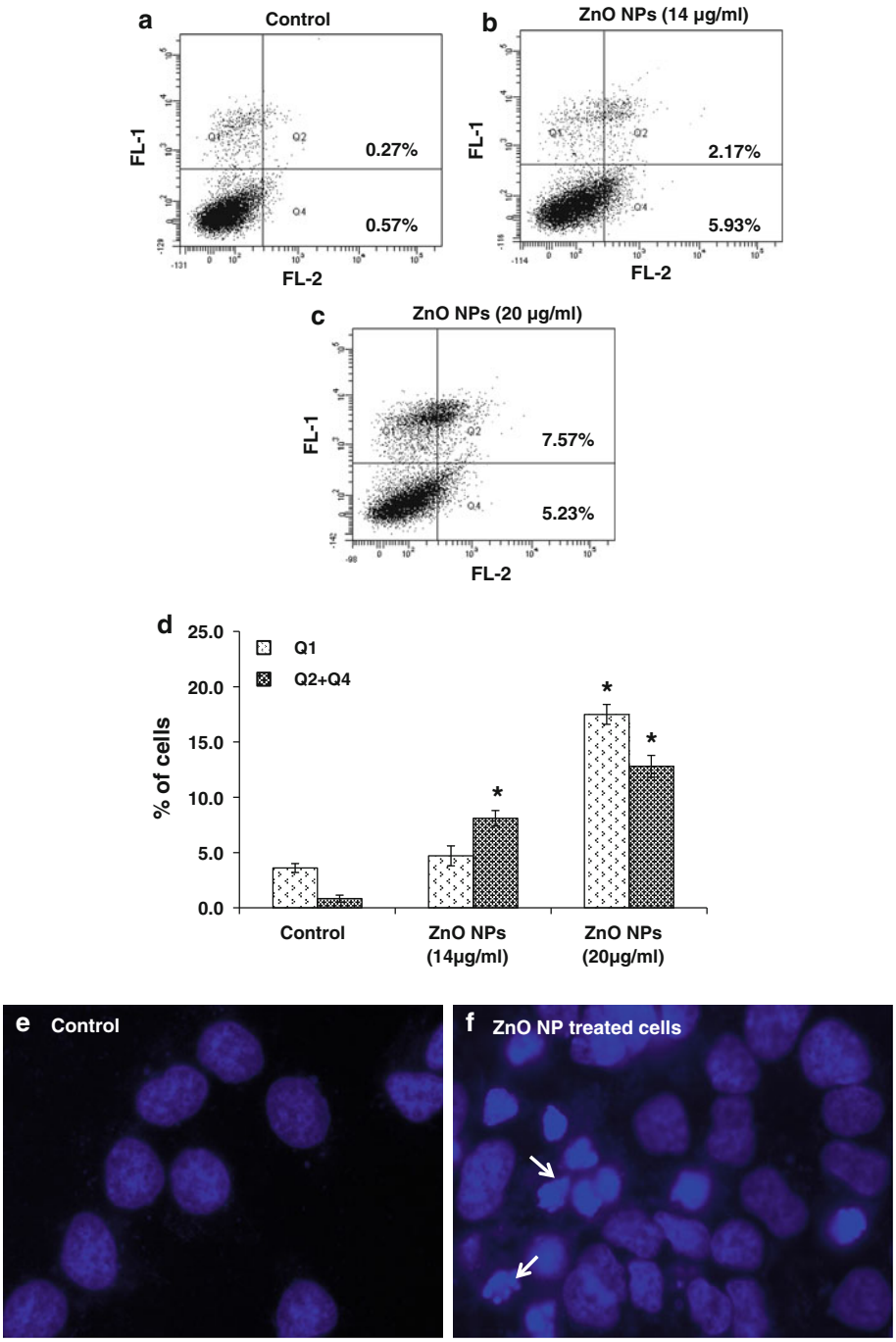

Fig. 6 ZnO NPs induced apoptosis in HepG2 cells: **a–d** Flow cytometric analysis of AnnexinV-FITC/PI stained cells. Data represent mean ± SEM of three experiments. $*p < 0.05$, compared to control. Representative dot plots of three independent experiments are presented; **e–f** Fluorescence images of cells stained with Hoechst 33342. ZnO NP treated cells show apoptotic cells with condensed or fragmented nuclei (indicated by *arrows*)

in human liver cells. Oxidative stress and not dissolution was found to be the underlying mechanism behind ZnO NP induced DNA damage and cell death. Our data also revealed that the mode of cell death was apoptosis which was mediated by the ROS triggered mitochondrial pathway as evidenced by decrease in MMP, modulation of Bax/Bcl2 ratio and cleavage of caspase-9. Finally, we also investigated the status and role of some major signaling molecules like MAPK and p53. Interestingly, JNK and p38 activation was observed, however, with minimal effect on ZnO NP induced cytotoxicity.

The characterization of ZnO NPs was done by DLS as well as TEM. However, the size obtained from DLS (267 nm) was more than the size measured by TEM (30 nm). This difference in size is due to the fact that different size determination methods give different results based on the principles employed—(1) DLS measures Brownian motion and subsequent size distribution of an

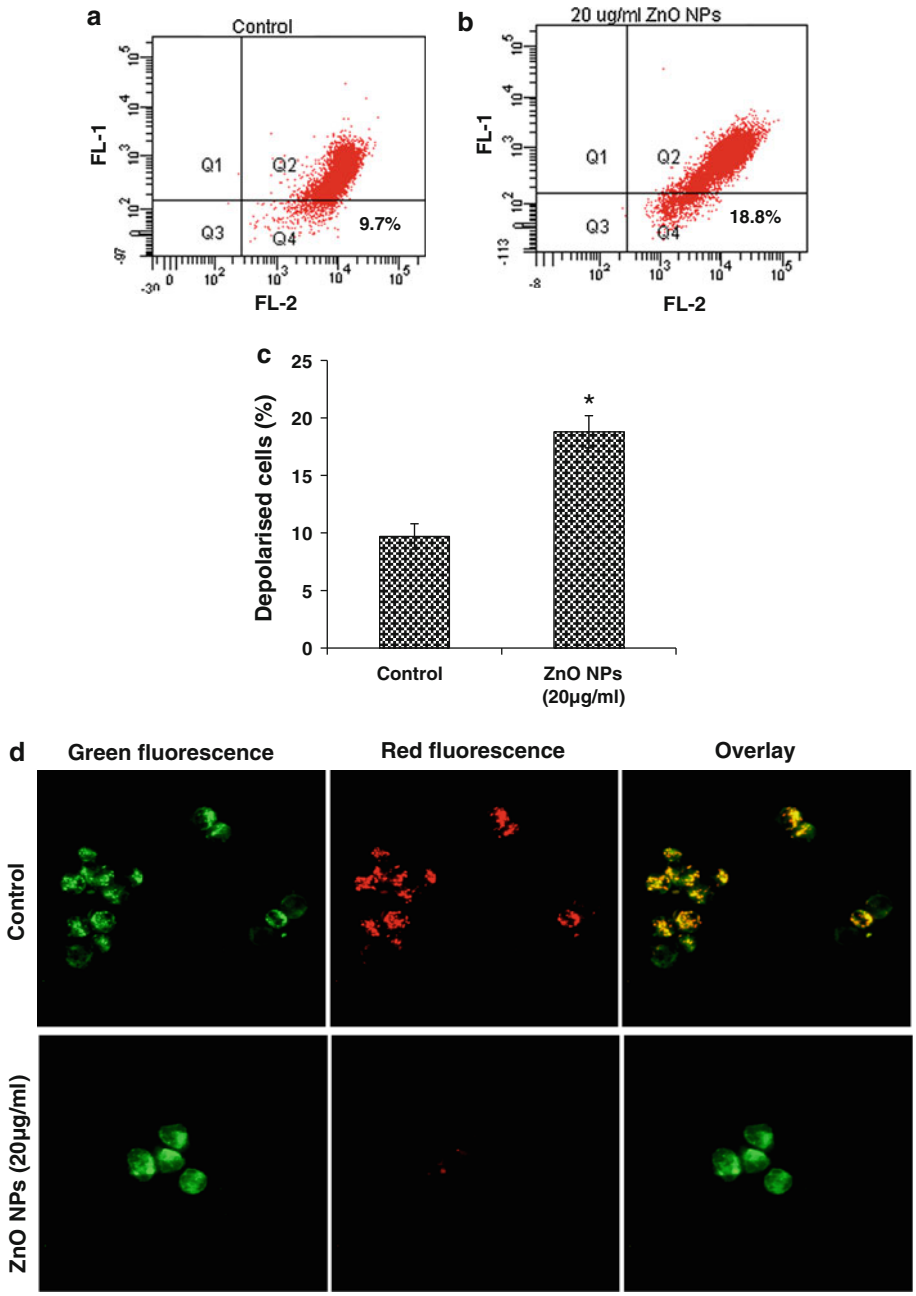

Fig. 7 ZnO NPs induced mitochondrial membrane potential (MMP) changes in HepG2 cells: **a–c** Flow cytometric analysis of JC-1 stained cells. Data represent mean ± SEM of three experiments. *$p < 0.05$, compared to control. Representative dot plots of three independent experiments are presented; **d** Fluorescence images of ZnO NP induced changes in MMP in HepG2 cells. The first (*extreme left*) column showing only *green* fluorescence (aggregated form of JC-1), the second (*middle*) column showing only *red* fluorescence (monomeric form of JC-1), the third (*extreme right*) column showing *overlay* (*red–green* fluorescence)

ensemble collection of particles in solution and gives mean hydrodynamic diameter which is usually larger than TEM diameter as it includes a few solvent layers (2) during DLS measurement there is a tendency of particles to agglomerate in the aqueous state thereby giving the size of clustered particles rather than individual particles (3) it reports an intensity weighted average hydrodynamic diameter of a collection of particles so any polydispersity of the sample will skew the average diameter towards larger particle sizes [32].

The interference of some nanomaterials with commonly used cytotoxicity test systems has been well documented in the literature [33, 34]. Therefore, it has been suggested that the cytotoxicity of nanomaterials should be assessed with two or more independent test systems for validating the findings [33, 34]. We have evaluated the cytotoxicity of ZnO NPs by three different assay systems viz. the MTT assay, NR uptake and the LDH release assay to increase the reliability of the data. The assays revealed a cytotoxic potential of ZnO NPs at 14 and 20 µg/ml after 12 and 24 h exposure in HepG2 cells.

Oxidative stress is the most discussed paradigm for the toxicity of NPs. This has been attributed to their small size and hence large surface area which is generally thought to

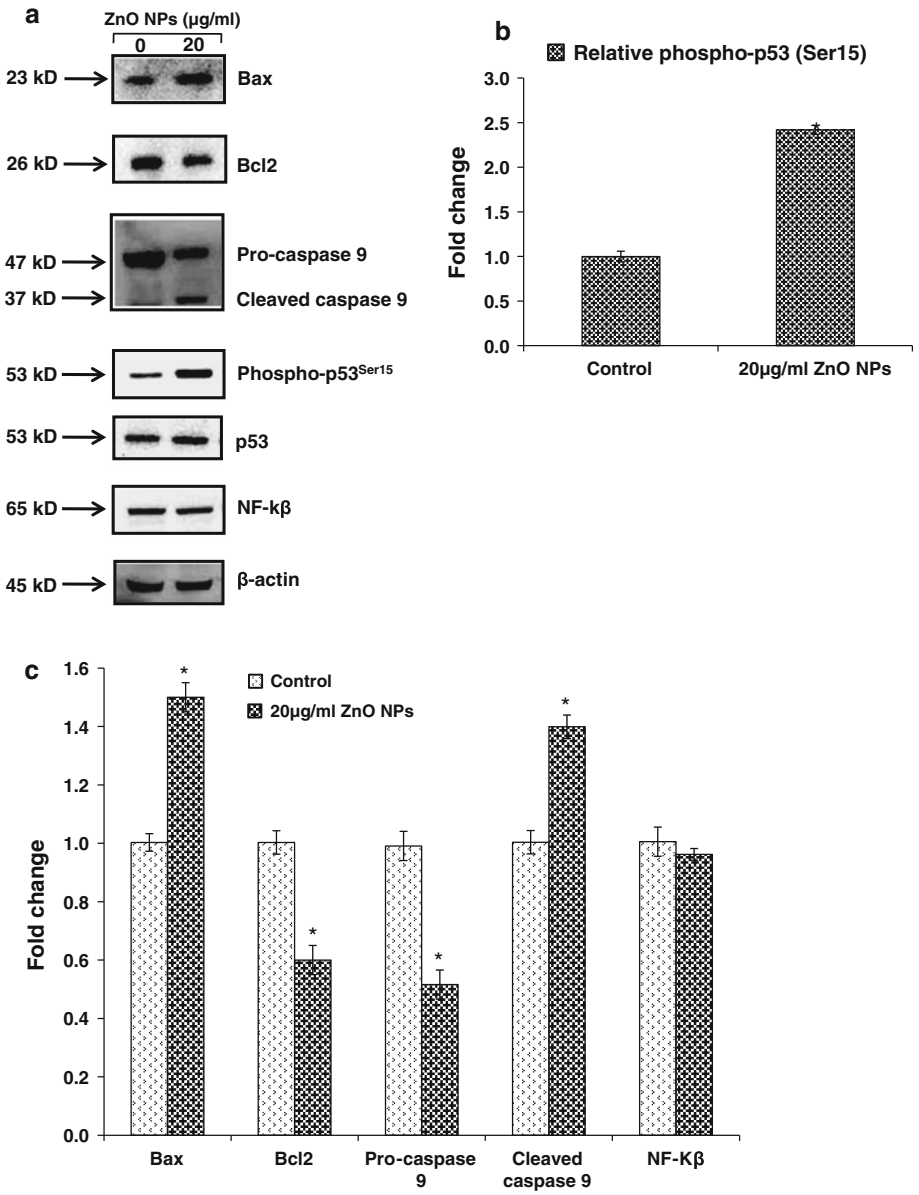

Fig. 8 Western blot analysis of proteins involved in apoptosis: **a** Bax, Bcl2, NF-kβ expression levels, caspase-9 activation and $p53^{Ser15}$ phosphorylation. β-actin was used as internal control to normalize the data; **c–d** Relative quantification of protein expression levels. Data represent mean ± SEM of three experiments. *$p < 0.05$, compared to control

produce ROS and oxidative stress [35]. The ZnO NPs in our study were also found to be capable of generating intracellular ROS when examined by the cell permeable dye DCFH-DA. This observation is consistent with the earlier studies which have shown similar effects on primary mouse embryo fibroblast cells and human lymphoblastoid cells (WIL2-NS) [12, 36]. We also observed an increase in lipid peroxides in HepG2 cells on exposure to ZnO NPs, which represents another marker of oxidative stress. Lipid peroxidation can further give rise to more free radicals and damage biomolecules like DNA, protein and lipids in conjunction with ROS. It also causes injury to the cell membrane as indicated by an increased LDH release. Different ways for ROS generation by engineered nanoparticles have been proposed [35, 37]. The NPs can lead to spontaneous ROS generation at their surface owing to their chemical and surface characteristics. They can also lead to the generation of free radicals after their interaction with cellular components, e.g., mitochondrial damage. Another way by which ROS is generated is through the activation of NADPH-oxidase enzyme which is responsible for O_2^- production in the membrane of phagocytic cells. In case of ZnO NPs, the generation of ROS has been attributed to their semiconductor and nanolevel characteristic which leads to ROS generation even in the absence of light. The quality of ZnO nanocrystal decreases with size and results in increased interstitial zinc ions and oxygen vacancies [38, 39]. These crystal defects can lead to a large number of electron–hole pairs which can migrate to the nanoparticle surface and contribute to the ROS generation. The

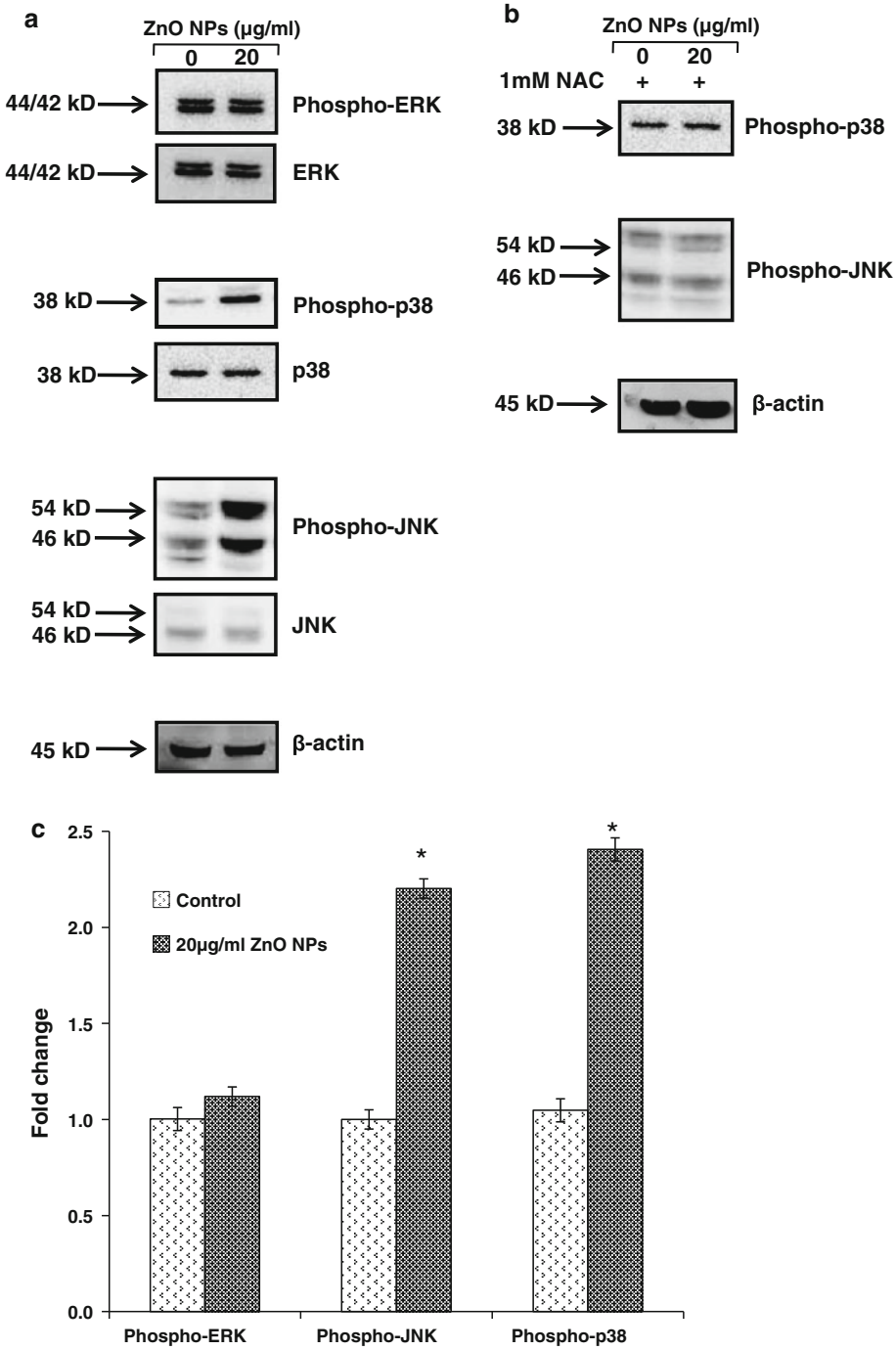

Fig. 9 Western blot analysis of proteins involved in MAPK signaling in HepG2 cells: **a** Effect of ZnO NPs exposure; **b** Effect of NAC on ZnO NP induced MAPK signaling; **c** Relative quantification of protein expression levels. Quantification was done using scion image software. Data represent mean ± SEM of three experiments. *$p < 0.05$, compared to control

electrons and holes can react with the oxygen and hydroxyl ions, respectively, present in the aqueous environment of ZnO NPs. This produces highly reactive free radicals including the superoxide anion radical (from electrons) and the hydroxyl radical (from holes) [5]. When in contact with the cellular environment, these radicals can oxidize and reduce macromolecules (DNA, lipids, proteins) resulting in significant oxidative damage to cell.

Some NPs owing to their small size are capable of reaching the nucleus and interact with DNA [40–42]. They may also exhibit an indirect effect on DNA through their ability to generate ROS [42]. This DNA damage may either lead to carcinogenesis or cell death, thus disrupting normal cell functions. We observed the genotoxic potential of ZnO NPs in HepG2 cells in the alkaline Comet assay which is capable of detecting single as well as double DNA strand breaks and alkali labile sites even at low levels of DNA damage [43]. Our earlier studies have also revealed the DNA damaging potential of these NPs in somatic cells (skin cells, lymphocytes) and germ cells [32, 44]. As ROS

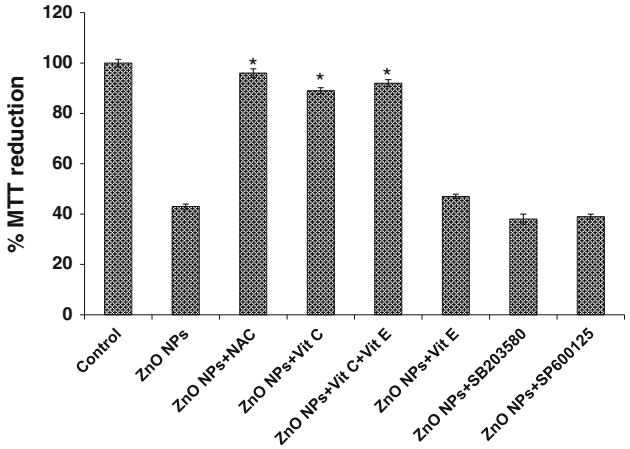

Fig. 10 Effect of MAPK inhibition, *N*-acetylcysteine, vitamins C and E on ZnO NPs induced cytotoxicity in HepG2 cells. Data represent mean ± SEM of three experiments. $^{*}p < 0.05$, compared to cell treated with only ZnO NPs

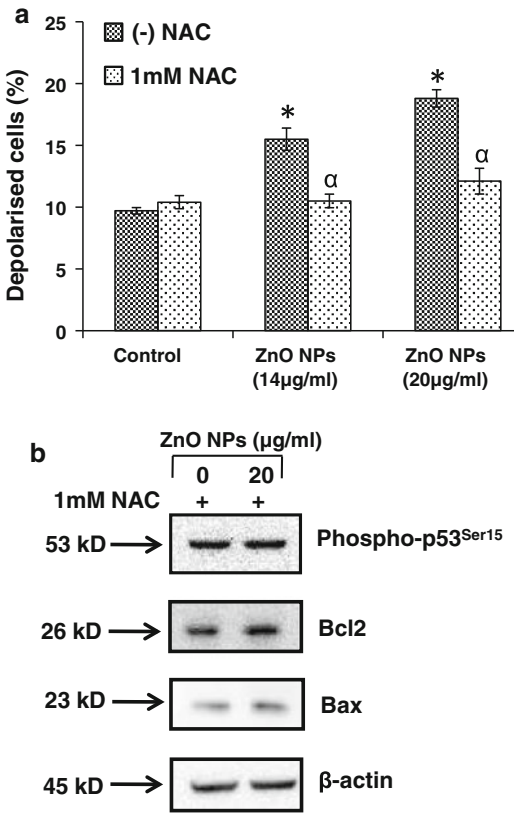

Fig. 11 Effect of *N*-acetylcysteine on mitochondrial mediated apoptosis **a** Effect of *N*-acetylcysteine on ZnO NPs induced loss of MMP. Data represent mean ± SEM of three experiments. $^{*}p < 0.05$ when compared to control. $^{\alpha}p < 0.05$ when compared to "without NAC" at the same concentration; **b** Effect of *N*-acetylcysteine on ZnO NPs induced Bax, Bcl_2 and p53 phosphorylation. *β*-actin was used as internal control to normalize the data. *Blots* shown are representative of three different experiments

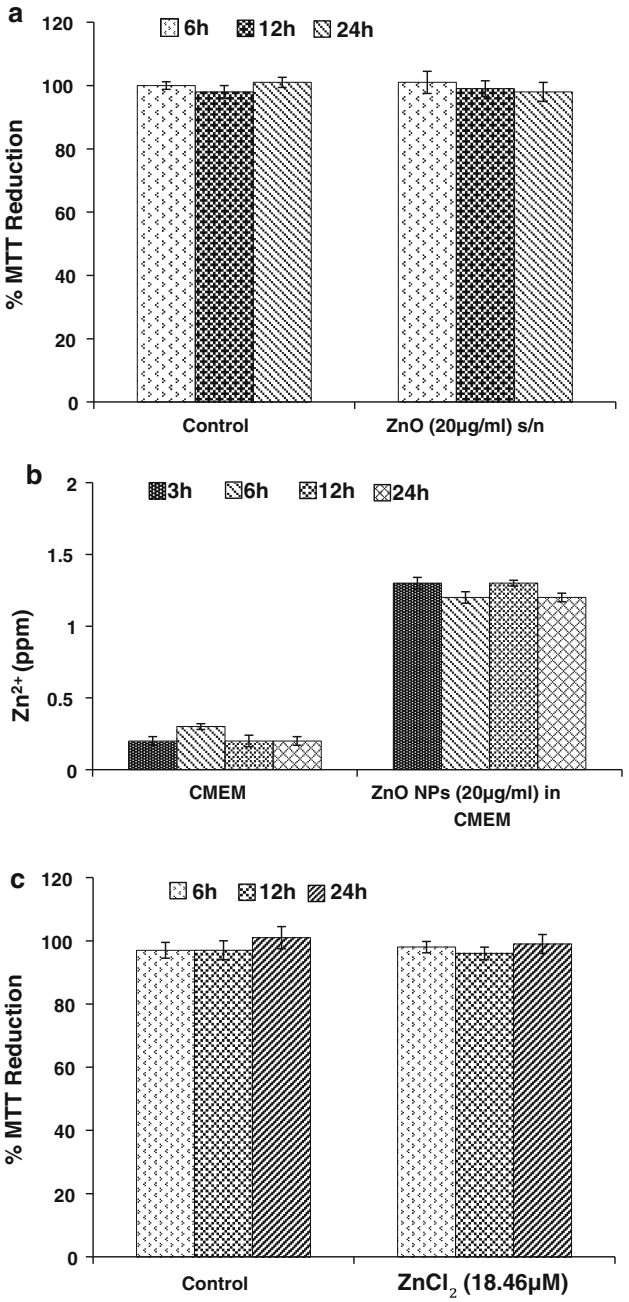

Fig. 12 Effect of dissolution on ZnO NPs induced cytotoxicity **a** Assessment of cytotoxicity of Zn^{2+} released into the medium from ZnO NPs; **b** Assessment of Zn^{2+} released from ZnO NPs; **c** Assessment of cytotoxicity of released Zn^{2+} using $ZnCl_2$ as the reference standard. The cytotoxicity was assessed by the MTT assay after 6, 12, and 24 h exposure. Data represent mean ± SEM of three experiments

are known to react with DNA molecule causing damage to both purine and pyrimidine bases as well as the DNA backbone [45], we investigated the link between oxidative stress and DNA damage in HepG2 cells via the Fpg modified Comet assay. The bacterial enzyme Fpg recognizes specifically the most common marker for DNA oxidation-8-oxo-7, 8-dihydroguanine (8-oxoGua). In the

present study, the level of Fpg-sensitive sites (oxidised purines) increased compared to the level of direct single strand breaks as observed in standard Comet assay. Moreover, NAC was able give protection against these ZnO NP induced DNA strand breaks and oxidative DNA damage. This confirms oxidative stress as the mediator of ZnO NP induced DNA damage. These results are in agreement with the findings of Karlsson et al. [46] who observed oxidative DNA lesions in cultured A549 cells after exposure to 20 μg/cm^2 (40 μg/ml) and 40 μg/cm^2 (80 μg/ml) ZnO NPs for 4 h.

The ZnO NP induced cell death observed in this study can occur by two distinct modes-apoptosis and necrosis which can be distinguished by morphological and biochemical features. Annexin V-FITC/PI staining of ZnO nanoparticle treated HepG2 cells resulted in an increase in Annexin$^+$/PI$^-$ and Annexin$^+$/PI$^+$ cells compared to the control (Annexin$^-$/PI$^-$) indicating apoptosis as a possible mode of cell death. To further confirm that ZnO NPs induced cell death represented apoptosis we examined the cells stained with Hoechst 33342 and found nuclear condensation and fragmentation which is another morphological hallmark of apoptosis.

ZnO NP exposure in HepG2 cells increased Bax protein levels with a corresponding decrease in Bcl2 protein expression. These Bcl2 family proteins play an important role in the mitochondrial pathway of apoptosis. Another key event in the intrinsic pathway is disruption of the mitochondrial transmembrane potential which results in the release of pro-apoptotic factors activating the caspase cascade [47]. We analyzed this crucial step of mitochondrial membrane depolarization in ZnO NP treated cells and found a collapse of $\Delta\Psi_m$ following treatment with ZnO NPs. We also observed the activation of caspase-9 as proved by a decrease in the pro-caspase level accompanied by an appearance of 37 kD cleavage product. Our results clearly demonstrate the role of mitochondria mediated pathway (intrinsic pathway) in ZnO NP induced apoptosis.

The MAPK pathways which consist of three main members, the extracellular signal-regulating kinase (ERK1/2), stress activated protein kinase (SAPK)/Jun-N-terminal kinase (JNK), and p38 are activated in response to various cellular stimuli such as oxidative stress [48]. The JNK pathway has been identified as a direct activator of the mitochondrial death machinery providing a molecular linkage from oxidative stress to the mitochondria mediated apoptosis. Therefore, we evaluated the link of MAPK with ROS production and apoptosis. We observed that the treatment of HepG2 cells with ZnO NPs caused JNK and p38 activation, however, the status of ERK remained unaltered. In addition, p38 and JNK activation was completely prevented in the presence of NAC suggesting that there is a ROS-dependent induction of JNK and p38 by ZnO NPs. These results point to the possibility that ROS—evoked JNK and p38 activation triggered the mitochondrial-dependent cell death pathway based on the well established role of these kinases in ROS mediated apoptosis [49]. Interestingly, inhibition of JNK and p-38 pathway by using their specific inhibitors (SP600125 and SB203580, respectively) did not protect cells from apoptosis. This shows that JNK and p38 kinases play no direct role in the apoptosis induced by ZnO NPs. However, their activation by ZnO NP generated ROS might be explained as an adaptive response to bypass the stress injury [50]. The importance of the MAPK cascade in NP induced cellular responses has not been explored much despite their multifunctional role in cell signaling especially under various stress conditions [48]. There is no study available on modulation of MAPK with ZnO NP exposure and this is the first to explore such effects.

DNA damage induces phosphorylation of tumor suppressor protein p53 at ser^{15} and activates it. This protein downregulates anti-apoptotic Bcl2 proteins and trans-activates puma, noxa and pro-apoptotic Bax to trigger the mitochondrial pathway of apoptosis. Therefore, the activation of p53 and a link between ROS and p53 activation was investigated. We observed an enhanced phosphorylation of p53 at ser^{15} on exposure to ZnO NPs which could be abrogated by NAC. This activation may be explained as a response to DNA damage which is caused by ZnO NPs induced ROS. We also sought to investigate the status of NFκB which is an important transcription factor controlling many important functions such as immunity, inflammation, and apoptosis [51]. There was no modulation in its expression in cells exposed to ZnO NPs.

To decipher the link between oxidative stress and ZnO NP induced toxicity in HepG2 cells, the cells were treated with ZnO NPs in the presence of NAC. NAC completely prevented ZnO NP induced apoptosis. It was also evaluated whether ROS targeted the mitochondria and thereby decreased the $\Delta\Psi_m$ in ZnO NP-treated HepG2 cells. Similarly, another antioxidant, vitamin C (ascorbic acid) exibited protective effects on cells treated with ZnO nanoparticles while vitamin E which is a well-known lipid peroxidation chainbreaking antioxidant was not very effective in preventing ZnO nanoparticle induced toxicity. We observed that a loss of MMP and an increased Bax/Bcl2 ratio induced by ZnO NP could also be inhibited in the presence of NAC. These results indicated that ROS caused the $\Delta\Psi_m$ loss, Bax/Bcl2 modulation and caspases activation, which accounted for the ZnO NP induced HepG2 apoptosis. A direct link between ROS and apoptosis is possible as ROS production causes dimerisation of Bax in the cytosol. This changes conformation of Bax exposing its mitochondrial docking motif leading to the translocation of Bax to mitochondria, channel formation

and the release of cytochrome c [18]. These results are supported by the findings of Heng et al. [52] who demonstrated that initial exposure of human bronchial epithelial cells (BEAS-2B) to oxidative stress increased their sensitivity to the cytotoxic potential of ZnO NPs.

In addition to apoptosis, autophagy is emerging as another important mechanism of cell death induced by the nanoparticles. Different types of nanoparticles have been found to induce autophagic cell death in human lung cells, dopaminergic neuronal cells and some studies have cited nanoparticle elicited ROS as the major stimulator of autophagy [53–55]. Oxidative stress activates transcription factors FOXO3 and NRF2 which positively regulate autophagy via stimulating the LC3, BNIP3 and p62 transcription [56]. ROS also inhibit ATG4 protease activity, thereby supporting autophagosome formation [56]. In addition to ROS, other major modulators of autophagy observed in our results are p53 and Bcl2. p53 transcriptionally activates several autophagy-related genes like DRAM, sestrins, AMPK [57]. Bcl2 is not only an anti-apoptosis protein but also an anti-autophagy protein. It interacts with the BH3 domain of Beclin1 protein, a key regulator of autophagy, thus inhibiting its autophagic function [57]. A significant decrease in Bcl2 levels observed in present study along with induction of P53 and ROS may also trigger autophagic cell death. However, the significance and relative contribution of autophagic/apoptotic cell death needs to be further investigated in future studies.

Some studies have raised doubt in ascribing the ZnO NPs toxicity to ROS or NPs per se and observed dissolution as the main cause [15]. Moreover, the phenomenon of dissolution is expected to become more prominent in the case of NPs due to its dependency on the surface area. The

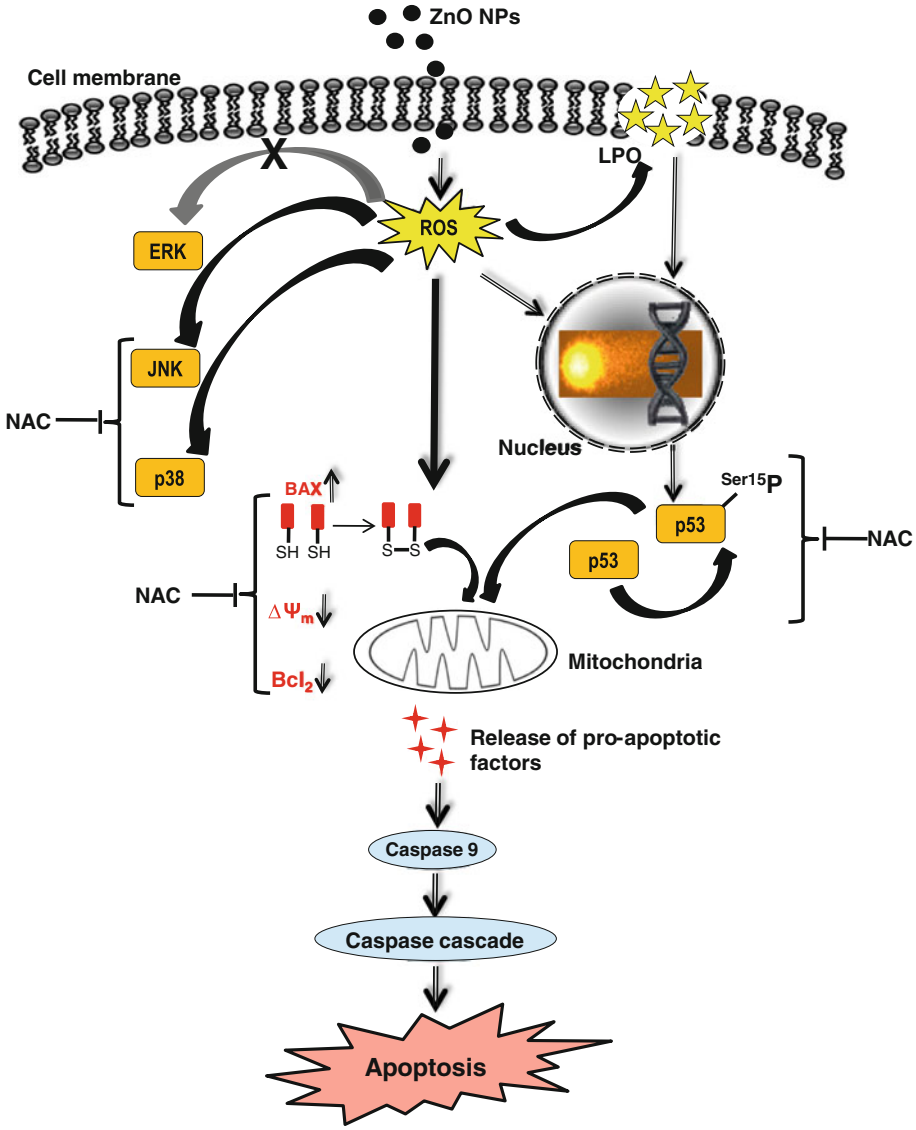

Fig. 13 Possible mechanisms involved in ZnO NP induced toxicity in human liver cells

toxicity of resulting metal ions is well known and accepted. Brunner et al. observed that more soluble NPs like ZnO and FeO showed greater cytotoxicity than insoluble NPs, such as CeO_2 and TiO_2 in human mesothelioma MSTO-211H and rodent 3T3 fibroblast cells; however, any correlation with the phenomenon of dissolution was not demonstrated experimentally [58]. Therefore, we addressed the probability of released Zn^{2+} contribution towards toxicity in our study by two different ways. We incubated cell culture media containing NPs at 37°C for 6, 12 and 24 h while mimicking the cell exposure conditions. The supernatant from this media did not result in toxicity at any time period discarding any contribution of released Zn^{2+} towards toxicity. To further understand the dissolution process taking place in our experimental conditions, we measured the Zn content in the supernatant by AAS. We found that the [Zn^{2+}] reached a level of 1.2 ppm in 6 h and remained constant for 12 and 24 h. Therefore, the maximum extent of dissolution that we got resulted in 3 h itself and remained constant for next 24 h showing that the liberation of Zn^{2+} from NPs is independent of time, in given conditions. We also attempted to answer the issue of dissolution by exposing cells to an appropriate reference material-$ZnCl_2$ at the Zn mass dose (18 μM) equimolar to Zn content in the supernatant. No decrease in cell viability was observed at 6, 12 and 24 h and this corroborated our results that the impact of Zn^{2+} release on toxicity is insignificant. This finding suggests that although the NPs release Zn^{2+} in the media, this amount is insufficient to cause toxicity. Therefore, the observed toxic responses on exposure to ZnO NPs are due to the NPs per se rather than the ions released from them. Our results are in agreement with those of Lin et al. [59] and Gojova et al. [11] who demonstrated that there is no ionic toxicity after ZnO NPs exposure, although it was done in different cellular systems and exposure conditions.

Conclusions

This is a significant study investigating the effects of ZnO NPs in human liver cells and exploring different mechanisms underlying their cytotoxic and genotoxic potential. HepG2 cells exposed to 14–20 μg/ml ZnO NPs showed a decrease in cell viability and the mode of ZnO NP induced cell death was found to be apoptosis. They also induced ROS generation, oxidative DNA damage evidenced by an increase in Fpg sensitive sites that could be prevented by NAC. Our results demonstrate that ROS triggered a decrease in MMP with a concomitant increase in the ratio of Bax/Bcl2 leading to mitochondrial mediated apoptosis. In addition, ZnO NPs activated p-38, JNK and induced $p53^{ser15}$ phosphorylation, however, the apoptosis was found to be independent of JNK and p38 pathways. Our results provide valuable insights into the mechanism of ZnO NP induced toxicity in human liver cells (Fig. 13).

Future investigations will focus on in vivo studies assessing the effects of ZnO nanoparticles in liver cells and elucidating their toxicity mechanism. Additionally, it would be of interest for further work to determine the role of TNF alpha and extrinsic apoptotic pathway in ZnO NP induced apoptosis.

Acknowledgments The authors thank CSIR, New Delhi for funding under its network project (NWP35) and supra institutional project (SIP-08). The funding from the Department of Science and Technology under the nanomission project—DST-NSTI grant (SR/S5/NM-01/2007) and UK India Education and Research Initiative (UKIERI) standard award to Indian Institute of Toxicology Research, Lucknow, India (DST/INT/UKIERI/SA/P-10/2008) and University of Bradford, Bradford, UK (SA 07-067) is duly acknowledged. The funding for the NanoLINEN project from the Department of Biotechnology, Government of India, under the NewINDIGO scheme is also acknowledged. Vyom Sharma thanks the Council of Scientific and Industrial Research (New Delhi) for the award of a Senior Research Fellowship.

Conflict of interest The authors declare that there is no conflict of interest.

References

1. Schilling K, Bradford B, Castelli D, Dufour E, Nash JF, Pape W et al (2010) Human safety review of "nano" titanium dioxide and zinc oxide. Photochem Photobiol Sci 9(4):495–509. doi:10.1039/b9pp00180h
2. Gerloff K, Albrecht C, Boots AW, Förster I, Schins RPF (2009) Cytotoxicity and oxidative DNA damage by nanoparticles in human intestinal Caco-2 cells. Nanotoxicology 3(4):355–364
3. Jin T, Sun D, Su JY, Zhang H, Sue HJ (2009) Antimicrobial efficacy of zinc oxide quantum dots against Listeria monocytogenes, *Salmonella Enteritidis*, and *Escherichia coli* O157:H7. J Food Sci 74(1):M46–M52. doi:10.1111/j.1750-3841.2008.01013.x
4. He L, Liu Y, Mustapha A, Lin M (2010) Antifungal activity of zinc oxide nanoparticles against *Botrytis cinerea* and *Penicillium expansum*. Microbiol Res. doi:10.1016/j.micres.2010.03.003
5. Rasmussen JW, Martinez E, Louka P, Wingett DG (2010) Zinc oxide nanoparticles for selective destruction of tumor cells and potential for drug delivery applications. Expert Opin Drug Deliv 7(9):1063–1077. doi:10.1517/17425247.2010.502560
6. John S, Marpu S, Li J, Omary M, Hu Z, Fujita Y et al (2010) Hybrid zinc oxide nanoparticles for biophotonics. J Nanosci Nanotechnol 10(3):1707–1712
7. Miller RJ, Lenihan HS, Muller EB, Tseng N, Hanna SK, Keller AA (2003) Impacts of metal oxide nanoparticles on marine phytoplankton. Environ Sci Technol 44(19):7329–7334. doi:10.1021/es100247x
8. Sinha R, Karan R, Sinha A, Khare SK (2010) Interaction and nanotoxic effect of ZnO and Ag nanoparticles on mesophilic and halophilic bacterial cells. Bioresour Technol. doi:10.1016/j.biortech.2010.07.117

9. Wang HJ, Growcock AC, Tang TH, O'Hara J, Huang YW, Aronstam RS (2010) Zinc oxide nanoparticle disruption of store-operated calcium entry in a muscarinic receptor signaling pathway. Toxicol In Vitro 24(7):1953–1961. doi:10.1016/j.tiv.2010.08.005
10. Wang B, Feng W, Wang M, Wang T, Gu T, Zhu M et al (2008) Acute toxicological impact of nano- and submicro-scaled zinc oxide powder on healthy adult mice. J Nanopart Res 10:263–276. doi:10.1007/s11051-007-9245-3
11. Gojova A, Guo B, Kota RS, Rutledge JC, Kennedy IM, Barakat AI (2007) Induction of inflammation in vascular endothelial cells by metal oxide nanoparticles: effect of particle composition. Environ Health Perspect 115(3):403–409. doi:10.1289/ehp8497
12. Yang H, Liu C, Yang D, Zhang H, Xi Z (2009) Comparative study of cytotoxicity, oxidative stress and genotoxicity induced by four typical nanomaterials: the role of particle size, shape and composition. J Appl Toxicol 29(1):69–78. doi:10.1002/jat.1385
13. Osman IF, Baumgartner A, Cemeli E, Fletcher JN, Anderson D (2010) Genotoxicity and cytotoxicity of zinc oxide and titanium dioxide in HEp-2 cells. Nanomedicine (Lond) 5(8):1193–1203. doi:10.2217/nnm.10.52
14. George S, Pokhrel S, Xia T, Gilbert B, Ji Z, Schowalter M et al (2009) Use of a rapid cytotoxicity screening approach to engineer a safer zinc oxide nanoparticle through iron doping. ACS Nano 4(1):15–29. doi:10.1021/nn901503q
15. Franklin NM, Rogers NJ, Apte SC, Batley GE, Gadd GE, Casey PS (2007) Comparative toxicity of nanoparticulate ZnO, bulk ZnO, and $ZnCl_2$ to a freshwater microalga (*Pseudokirchneriella subcapitata*): the importance of particle solubility. Environ Sci Technol 41(24):8484–8490
16. Moos PJ, Chung K, Woessner D, Honeggar M, Cutler NS, Veranth JM (2010) ZnO particulate matter requires cell contact for toxicity in human colon cancer cells. Chem Res Toxicol 23(4):733–739. doi:10.1021/tx900203v
17. Cadet J, Douki T, Ravanat JL (2010) Oxidatively generated base damage to cellular DNA. Free Radic Biol Med 49(1):9–21. doi:10.1016/j.freeradbiomed.2010.03.025
18. Neuzil J, Wang XF, Dong LF, Low P, Ralph SJ (2006) Molecular mechanism of 'mitocan'-induced apoptosis in cancer cells epitomizes the multiple roles of reactive oxygen species and Bcl-2 family proteins. FEBS Lett 580(22):5125–5129. doi:10.1016/j.febslet.2006.05.072
19. Navarro R, Busnadiego I, Ruiz-Larrea MB, Ruiz-Sanz JI (2006) Superoxide anions are involved in doxorubicin-induced ERK activation in hepatocyte cultures. Ann N Y Acad Sci 1090:419–428. doi:10.1196/annals.1378.045
20. Oberdorster G, Oberdorster E, Oberdorster J (2005) Nanotoxicology: an emerging discipline evolving from studies of ultrafine particles. Environ Health Perspect 113(7):823–839. doi:10.1289/ehp7339
21. Chen Z, Meng H, Yuan H, Xing G, Chen C, Zhao F et al (2007) Identification of target organs of copper nanoparticles with ICP-MS technique. J Radioanal Nucl Chem 272(3):599–603
22. Yamago S, Tokuyama H, Nakamura E, Kikuchi K, Kananishi S, Sueki K et al (1995) In vivo biological behavior of a water-miscible fullerene: 14C labeling, absorption, distribution, excretion and acute toxicity. Chem Biol 2(6):385–389
23. Suzuki H, Toyooka T, Ibuki Y (2007) Simple and easy method to evaluate uptake potential of nanoparticles in mammalian cells using a flow cytometric light scatter analysis. Environ Sci Technol 41(8):3018–3024
24. Mosmann T (1983) Rapid colorimetric assay for cellular growth and survival: application to proliferation and cytotoxicity assays. J Immunol Methods 65(1–2):55–63. doi:10.1016/0022-1759(83)90303-4
25. Reed LJ, Muench H (1938) A simple method of estimating fifty percent endpoints. Am J Hy 27:493–497
26. Borenfreund E, Puerner JA (1985) Toxicity determined in vitro by morphological alterations and neutral red absorption. Toxicol Lett 24(2–3):119–124
27. Wan CP, Myung E, Lau BH (1993) An automated micro-fluorometric assay for monitoring oxidative burst activity of phagocytes. J Immunol Methods 159(1–2):131–138. doi:10.1016/0022-1759(93)90150-6
28. Bajpayee M, Pandey AK, Parmar D, Mathur N, Seth PK, Dhawan A (2005) Comet assay responses in human lymphocytes are not influenced by the menstrual cycle: a study in healthy Indian females. Mutat Res 565(2):163–172. doi:10.1016/j.mrgentox.2004.10.008
29. Tice RR, Agurell E, Anderson D, Burlinson B, Hartmann A, Kobayashi H et al (2000) Single cell gel/comet assay: guidelines for in vitro and in vivo genetic toxicology testing. Environ Mol Mutagen 35(3):206–221. doi:10.1002/(SICI)1098-2280(2000)35:3
30. Smith CC, O'Donovan MR, Martin EA (2006) hOGG1 recognizes oxidative damage using the comet assay with greater specificity than FPG or ENDOIII. Mutagenesis 21(3):185–190. doi:10.1093/mutage/gel019
31. Bradford MM (1976) A rapid and sensitive method for the quantitation of microgram quantities of protein utilizing the principle of protein-dye binding. Anal Biochem 72:248–254. doi:10.1016/0003-2697(76)90527-3
32. Sharma V, Shukla RK, Saxena N, Parmar D, Das M, Dhawan A (2009) DNA damaging potential of zinc oxide nanoparticles in human epidermal cells. Toxicol Lett 185(3):211–218. doi:10.1016/j.toxlet.2009.01.008
33. Dhawan A, Sharma V (2010) Toxicity assessment of nanomaterials: methods and challenges. Anal Bioanal Chem 398(2):589–605. doi:10.1007/s00216-010-3996-x
34. Monteiro-Riviere NA, Inman AO, Zhang LW (2009) Limitations and relative utility of screening assays to assess engineered nanoparticle toxicity in a human cell line. Toxicol Appl Pharmacol 234(2):222–235. doi:10.1016/j.taap.2008.09.030
35. Xia T, Kovochich M, Brant J, Hotze M, Sempf J, Oberley T et al (2006) Comparison of the abilities of ambient and manufactured nanoparticles to induce cellular toxicity according to an oxidative stress paradigm. Nano Lett 6(8):1794–1807. doi:10.1021/nl061025k
36. Yin H, Casey PS, McCall MJ, Fenech M (2010) Effects of surface chemistry on cytotoxicity, genotoxicity, and the generation of reactive oxygen species induced by ZnO nanoparticles. Langmuir 26(19):15399–15408. doi:10.1021/la101033n
37. Song W, Zhang J, Guo J, Ding F, Li L, Sun Z (2009) Role of the dissolved zinc ion and reactive oxygen species in cytotoxicity of ZnO nanoparticles. Toxicol Lett 199(3):389–397
38. Nel A, Xia T, Madler L, Li N (2006) Toxic potential of materials at the nanolevel. Science 311(5761):622–627
39. Sharma SK, Pujari PK, Sudarshan K, Dutta D, Mahapatra M, Godbole SV et al (2009) Positron annihilation studies in ZnO nanoparticles. Solid State Commun 149:550–554
40. Chen M, von Mikecz A (2005) Formation of nucleoplasmic protein aggregates impairs nuclear function in response to SiO_2 nanoparticles. Exp Cell Res 305(1):51–62. doi:10.1016/j.yexcr.2004.12.021
41. Sharma V, Singh SK, Anderson D, Tobin DJ, Dhawan A (2011) Zinc oxide nanoparticle induced genotoxicity in primary human epidermal keratinocytes. J Nanosci Nanotechnol 11(5):3782–3788
42. Shukla RK, Sharma V, Pandey AK, Singh S, Sultana S, Dhawan A (2010) ROS-mediated genotoxicity induced by titanium

dioxide nanoparticles in human epidermal cells. Toxicol In Vitro 25:231–241
43. Collins AR (2004) The comet assay for DNA damage and repair: principles, applications, and limitations. Mol Biotechnol 26(3):249–261. doi:10.1385/MB:26:3:249
44. Gopalan RC, Osman IF, Amani A, De Matas M, Anderson D (2009) The effect of zinc oxide and titanium dioxide nanoparticles in the Comet assay with UVA photoactivation of human sperm and lymphocytes. Nanotoxicology 3(1):33–39. doi:10.1080/17435390802596456
45. Martinez GR, Loureiro AP, Marques SA, Miyamoto S, Yamaguchi LF, Onuki J et al (2003) Oxidative and alkylating damage in DNA. Mutat Res 544(2–3):115–127. doi:10.1016/j.mrrev.2003.05.005
46. Karlsson HL, Cronholm P, Gustafsson J, Moller L (2008) Copper oxide nanoparticles are highly toxic: a comparison between metal oxide nanoparticles and carbon nanotubes. Chem Res Toxicol 21(9):1726–1732. doi:10.1021/tx800064j
47. Elmore S (2007) Apoptosis: a review of programmed cell death. Toxicol Pathol 35(4):495–516. doi:10.1080/01926230701320337
48. Chang L, Karin M (2001) Mammalian MAP kinase signalling cascades. Nature 410(6824):37–40. doi:10.1038/35065000
49. Aoki H, Kang PM, Hampe J, Yoshimura K, Noma T, Matsuzaki M et al (2002) Direct activation of mitochondrial apoptosis machinery by c-Jun N-terminal kinase in adult cardiac myocytes. J Biol Chem 277(12):10244–10250. doi:10.1074/jbc.M112355200
50. El-Najjar N, Chatila M, Moukadem H, Vuorela H, Ocker M, Gandesiri M et al (2010) Reactive oxygen species mediate thymoquinone-induced apoptosis and activate ERK and JNK signaling. Apoptosis 15(2):183–195. doi:10.1007/s10495-009-0421-z
51. Gilmore TD (1999) The Rel/NF-kappaB signal transduction pathway: introduction. Oncogene 18(49):6842–6844. doi:10.1038/sj.onc.1203237
52. Heng BC, Zhao X, Xiong S, Ng KW, Boey FY, Loo JS (2010) Toxicity of zinc oxide (ZnO) nanoparticles on human bronchial epithelial cells (BEAS-2B) is accentuated by oxidative stress. Food Chem Toxicol 48(6):1762–1766. doi:10.1016/j.fct.2010.04.023
53. Afeseh Ngwa H, Kanthasamy A, Gu Y, Fang N, Anantharam V, Kanthasamy AG (2011) Manganese nanoparticle activates mitochondrial dependent apoptotic signaling and autophagy in dopaminergic neuronal cells. Toxicol Appl Pharmacol 256(3):227–240. doi:10.1016/j.taap.2011.07.018
54. Khan MI, Mohammad A, Patil G, Naqvi SA, Chauhan LK, Ahmad I (2012) Induction of ROS, mitochondrial damage and autophagy in lung epithelial cancer cells by iron oxide nanoparticles. Biomaterials 33(5):1477–1488. doi:10.1016/j.biomaterials.2011.10.080
55. Li JJ, Hartono D, Ong CN, Bay BH, Yung LY (2010) Autophagy and oxidative stress associated with gold nanoparticles. Biomaterials 31(23):5996–6003. doi:10.1016/j.biomaterials.2010.04.014
56. Scherz-Shouval R, Elazar Z (2011) Regulation of autophagy by ROS: physiology and pathology. Trends Biochem Sci 36(1):30–38. doi:10.1016/j.tibs.2010.07.007
57. Morselli E, Galluzzi L, Kepp O, Marino G, Michaud M, Vitale I et al (2011) Oncosuppressive functions of autophagy. Antioxid Redox Signal 14(11):2251–2269. doi:10.1089/ars.2010.3478
58. Brunner TJ, Wick P, Manser P, Spohn P, Grass RN, Limbach LK et al (2006) In vitro cytotoxicity of oxide nanoparticles: comparison to asbestos, silica, and the effect of particle solubility. Environ Sci Technol 40(14):4374–4381
59. Lin W, Xu Y, Huang C, Ma Y, Shannon KB, Chen D et al (2009) Toxicity of nano- and micro-sized ZnO particles in human lung epithelial cells. J Nanopart Res 11:25–39. doi:10.1007/s11051-008-9419-7